Concerted Thermal Cycloreversion of Unsaturated Azo *N*-Oxides[1]

Henrik Olsen and James P. Snyder*

Contribution from the Department of General and Organic Chemistry, H. C. Ørsted Institute, University of Copenhagen, DK-2100 Copenhagen Ø, Denmark. *July 20, 1976*

Abstract: The synthesis of a series of polycyclic, unsaturated azo *N*-oxides and attempts to convert them under mild conditions to the corresponding azoalkanes is described. The *N*-oxides decompose thermally to N_2O and a hydrocarbon diene. Evaluation of the kinetics of the fragmentation as a function of azo *N*-oxide structure and solvent permits the conclusion that the reaction proceeds by an unsymmetrical but concerted pathway. Analysis of the relative rate and activation parameter solvent dependence suggests that the transition state is less polar than the ground state and that the reaction as a whole is entropy controlled. Furthermore, two cases in which cyclobutane rings seem to participate in the cycloreversion are discussed. Semiempirical potential energy surface calculations for the N_2 and N_2O extrusion reactions of 2,3-diazabicyclo[2.2.1]hepta-2,5-diene and the corresponding *N*-oxide have been performed with geometry optimization. The results parallel closely mechanistic inferences drawn from the kinetic studies; however, they do not account for the great difference in decomposition rates between comparable azo and azoxy bicycles ($k_{azo}/k_{azoxy} \simeq 10^{17}$).

Small molecular fragments such as CO, SO, SO_2, N_2, and N_2O when incorporated in a suitable carbon skeleton can be extruded to produce the corresponding hydrocarbon.[2] Nitrogen extrusion has received the greatest attention, probably because the starting materials are readily accessible and, most important, because the reaction is often spontaneous. Thus a wide variety of unusual or strained structures have been prepared under gentle conditions by employing N_2 release as a last synthetic step.[3]

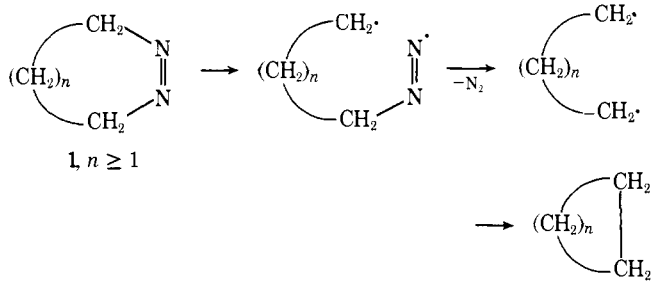

1, $n \geq 1$

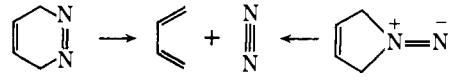

2 **3**

Deazetation has likewise contributed greatly to our understanding of reaction pathways. From the thermal destruction of saturated azoalkanes such as **1**, biradical intermediates may be inferred or observed on the higher reaches of the singlet potential energy surface.[4] The influence of light has likewise provided information about the triplet species and other excited states.[5]

Alternatively unsaturated precursors, for example, azoalkane **2**[6,7] and diazene **3**,[8] appear to decompose in a single step whereby both C–N bonds cleave simultaneously in concert

Scheme I

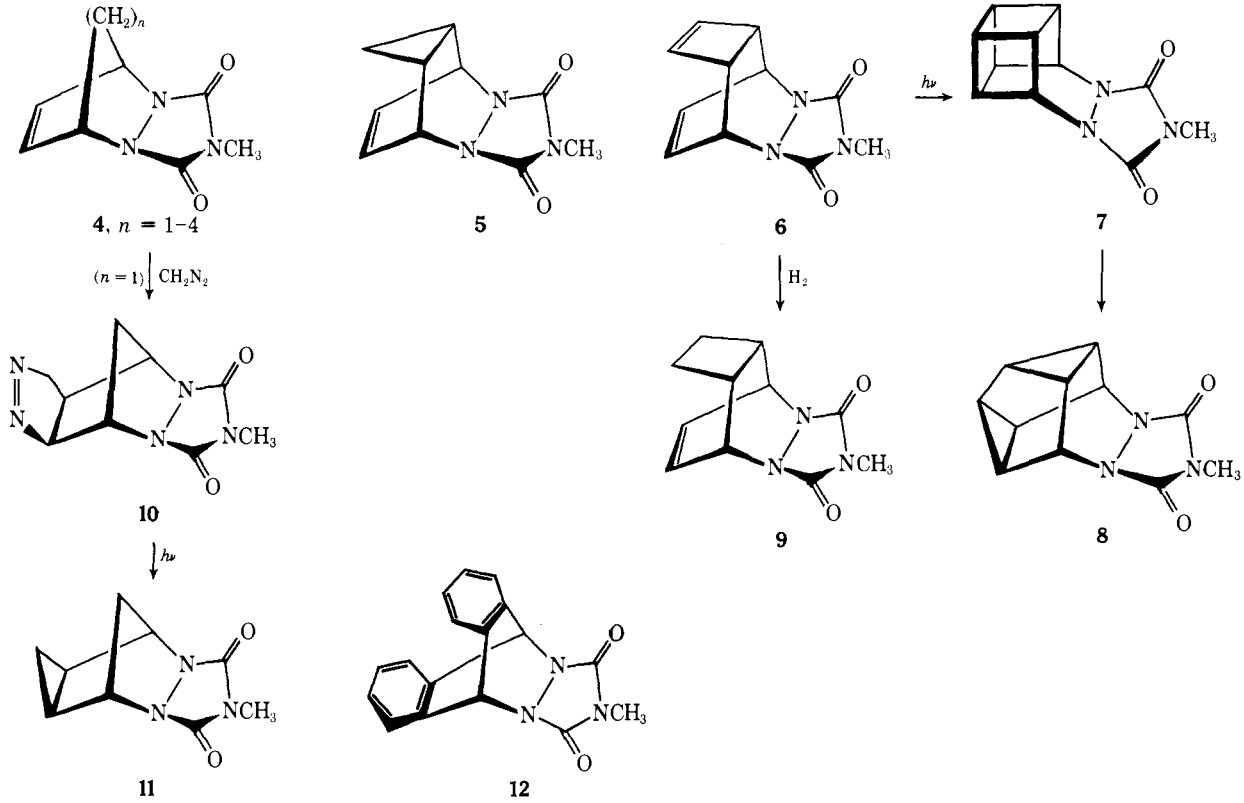

with bond formation in the product fragments. By replacement of the C=C double bonds in **2** and **3** with a three-[7,9,10] and in some cases a four-membered ring,[11] a similar result obtains. The facility and homogeneity of the reaction has led Berson and his co-workers to propose several "concertedness" criteria for retrocycloaddition.[12]

Recently we reported the parallel thermal extrusion of N_2O from a series of unsaturated polycycles analogous to **2**.[13] The relative rate differences for N_2 vs. N_2O loss are enormous although both processes appear to fulfill the pericyclic requirements. In the current study we present additional kinetic data and the results of SCF-MO potential energy surface calculations for the N_2 and N_2O extrusions.

Synthesis. As precursors to the unsaturated azo *N*-oxides we have employed the corresponding *N*-methyltriazolinedione (MTAD) adducts. Compounds **4–6** were reported previously[14] while the remainder, **7–9, 11, 12,** are obtained by the Diels-Alder reaction of MTAD and a suitable diene and by the well-known reactions outlined in Scheme I.

The polycyclic, unsaturated azoxyalkanes **14–21** have been

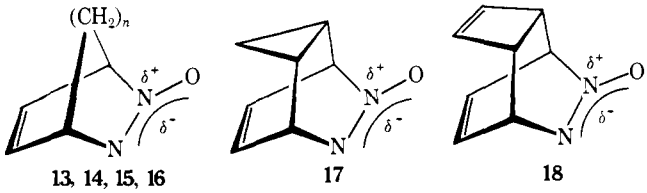

13, 14, 15, 16
n = 1, 2, 3, 4

17

18

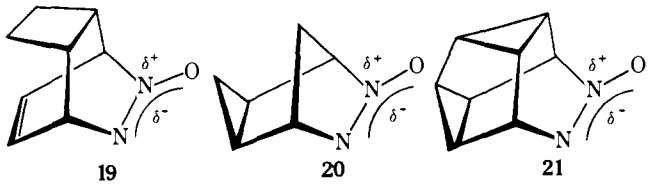

19 **20** **21**

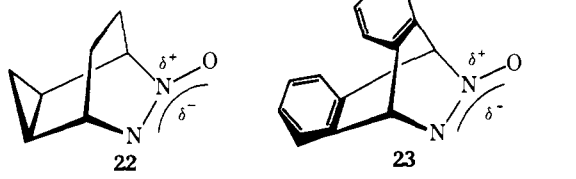

22 **23**

prepared by treatment of the MTAD adducts with high concentrations of KOH and 35% hydrogen peroxide in water or ethylene glycol/water at 40–100 °C. The reaction medium is essentially that used previously for synthesis of the corresponding saturated azo *N*-oxides.[14] Yields in the present series, however, are much more sensitive to temperature, reaction time, and KOH/adduct ratio than was found for the latter. A particularly critical case is the unsaturated, cyclopropyl derivative **17**. Since this compound thermolyzes rapidly above 50 °C, the hydrolytic oxidation must proceed between 35–45 °C. Above 45 °C the yield (70%) drops drastically, while below 35 °C adduct **5** is imperceptibly transformed over long periods of time. Optimum conditions for synthesis of *N*-oxides **14–21** are listed in Chart I in the Experimental Section; yields and other physical data, in Table I.

Several attempts were made to prepare the bicycloheptadiene *N*-oxide **13** and the anthracene derivative **23.** In the former case oxidative hydrolysis in various mixtures of water and ethylene glycol led only to the formation of cyclopentadiene. At 20 °C the starting adduct **4** (n = 1) disappeared slowly, whereas at 30–40 °C it reacted completely within half an hour. There is no obvious reason for supposing that methylurazole **4** reacts differently from the other adducts. Consequently we conclude that *N*-oxide **13** was formed, but is thermally labile at the lowest temperature required for its preparation. This behavior is consistent with the relatively great strain incorporated in the diazabicycloheptadiene skeleton.[15] Moreover, as shall be discussed in more detail below, molecular models indicate that the C=C bond in **13** is very favorably disposed for assisting the elimination of N_2O in a pericyclic transition state.

The dibenzo adduct **12** proved to be highly insoluble in the polar $OH^-/H_2O_2/H_2O$ medium. At temperatures below 50 °C no reaction occurred in the heterogeneous mixture. At higher temperatures oxidative hydrolysis undoubtedly sets in, but no azo *N*-oxide could be isolated. Again we postulate that N_2O extrusion is more effective than azoxy formation.

The structure of the *N*-oxides follows from their spectroscopic properties (Table I), formation by oxidation,[15,16] and reduction by hexachlorodisilane.[17] In the infrared all compounds exhibit characteristic azoxy bands at 1200–1300 and 1480–1510.[14,18,19] Likewise the moderately intense first absorption maximum in the UV appears as expected from 230–245 nm.[14,18,20] The 60 MHz NMR spectra of the unsaturated series **14–21** are similar to those recorded for saturated azo *N*-oxides in that the α-bridgehead hydrogens appear together as a broad, diffuse singlet.[14] Significantly, at higher resolution decoupling experiments reveal small but decipherable chemical shift differences. Details of the high-resolution measurements will be reported separately.

Action of Hexachlorodisilane on Unsaturated Axo *N*-Oxides. It is well known that 3,6-dihydropyridazines (e.g., **2**) and their cyclopropyl derivatives extrude nitrogen rapidly and quantitatively.[7,9,10,21] For example, the azo compounds corresponding to *N*-oxides **14**,[6] **18**,[22] and **21**[9c] as well as the derivatives **24**[7] and **26**[23] have been generated from hydrazine

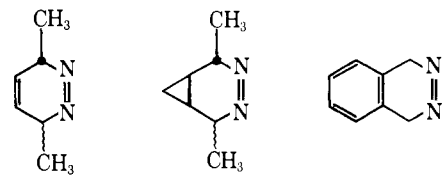

24 **25** **26**

precursors at temperatures ranging from −90 to −10 °C. With the single exception of **26,** none of the azoalkanes have been observed directly. Only nitrogen and the resulting hydrocarbon diene provide any historical clues. The cyclopropane functionalized azo systems corresponding to **20**,[9b] **22**,[9a] and **25**[10,12] can be isolated, but they too readily split out N_2 from 0 to 25 °C.

Since saturated bicyclic azo *N*-oxides are conveniently reduced to azoalkanes by $Cl_3SiSiCl_3$,[17] we considered the potential of the method for producing the labile unsaturated azo derivatives under mild conditions. Thus *N*-oxides **16, 18, 19,** and **21** were treated with the silicon reagent in an NMR probe at −78 °C and slowly warmed to room temperature with constant monitoring. At −40 °C the substrates were unchanged. However, from −35 to 0 °C all four compounds slowly disappeared, the *N*-oxide spectrum giving way exclusively to that of the corresponding hydrocarbon diene. Azo *N*-oxides **18** and **19** led to the bicyclic hydrocarbons **27** and **28,** respectively, whereas **21** yielded semibullvalene. No direct evidence for the presence of the desired azoalkanes, e.g., **29** and **30,** could be gathered. Thermal decomposition is clearly much more rapid than silane reduction.

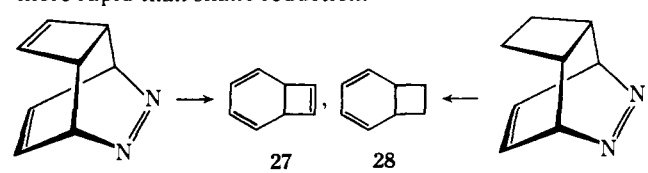

29 **27** **28** **30**

Table I. Yields and Physical Properties of Unsaturated and Highly Condensed *cis*-Azoxyalkanes

Compd	Yield, %[a]	Mp, deg (cryst solvent)	IR ($CHCl_3$) UV (96% EtOH) cm^{-1}	λ_{max}, nm (ϵ)	^1H NMR, τ (Me_4Si)[b]	Calcd/found C	H	N
14	82 (98)	48–49 (Et_2O)	1230, 1485	234 (5300)	3.46 (2 H, unsym t) 4.64 (2 H, broad m) 7.7–8.7 (4 H, m)	58.0/57.9	$C_6H_8N_2O$ 6.5/6.3	22.6/22.7
15	82 (100)	139–140 (Et_2O)	1287, 1500	236 (6500)	3.62 (2 H, m) 5.10 (2 H, broad s, hw = 13 Hz) 8.21 (6 H, m)	60.8/60.6	$C_7H_{10}N_2O$ 7.3/7.3	20.3/20.4
16	41 (53)	113–114 (Et_2O)	1303, 1502	234 (5900)	3.91 (2 H, m) 5.08 (2 H, broad s, hw = 12 Hz) 7.3–8.8 (8 H, broad m)	63.1/63.3	$C_8H_{12}N_2O$ 8.0/8.1	18.4/18.7
17	50 (70)	48–50 (Et_2O)	1280, 1500	241 (3200)	3.71 (2 H, t) 4.42 (2 H, m) 8.20 (2 H, m) 9.23 (2 H, m)	61.8/61.5	$C_7H_8N_2O$ 5.9/5.9	20.6/20.6
19	80 (100)	119–120 (Et_2O)	1267, 1291, 1498	237 (5000)	3.32 (2 H, t) 4.64 (2 H, broad s, hw = 10 Hz) 7.18 (2 H, m) 7.88 (2 H, m) 8.60 (2 H, m)	64.0/64.1	$C_8H_{10}N_{20}$ 6.7/7.0	19.2/19.2
18	65 (79)	101–102 (Et_2O)	1274, 1298, 1499	242 (3200)	3.70 (2 H, t) 3.91 (2 H, AB q) 4.70 (2 H, m) 6.83 (2 H, m)	64.9/64.9	$C_8H_8N_2O$ 5.4/5.4	19.0/18.9
20	65 (72)	60–61 (Et_2O–hexane)	1250, 1300, 1500	233 (5500)	5.32 (2 H, broad s, hw = 6 Hz) 8.1–9.2 (6 H, m)	58.1/58.0	$C_6H_8N_2O$ 6.5/6.7	22.6/22.7
21	70 (89)	(96% EtOH)	1252, 1312, 1500	234 (6100)	4.78 (2 H, q) 7.4–8.2 (6 H, m)	64.9/65.0	$C_8H_8N_2O$ 5.4/5.4	19.0/19.1

[a] Values in parentheses represent crude yields; those not in parentheses, recrystallized. Isolated materials in each case, however, possessed NMR spectra virtually identical with the analytical sample. [b] Solvent, $CDCl_3$.

In spite of the fact that the primary synthetic motivation for these experiments was frustrated, the correspondence between the character and rate of formation of the observed products and those derived by attempts to produce unsaturated species **2** by other routes[9c,22] confirms our structural assignment of **14–21** as azo *N*-oxides. Knowledge that the latter are simple oxides is essential for interpreting the kinetic data discussed below.

Retrocycloaddition of N_2O. Although unsaturated azoalkanes of which **2** is the prototype are generally incapable of being observed, the corresponding *N*-oxides **31** are isolable,

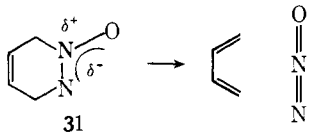

31

crystalline solids under ambient conditions. Increased temperatures, however, promote fragmentation in solution to hydrocarbon diene and N_2O in essentially quantitative yield.[13,17a]

The most labile *N*-oxide described in Table I is the cyclopropyl species **17.** The compound decomposes smoothly and quantitatively to cycloheptatriene above 35 °C as established by NMR, GLC, and the appropriate controls. Simultaneous release of N_2O was demonstrated by observing the growth of the characteristic NNO stretching vibrations at 2223 and 1285 cm^{-1} in the infrared.[24] The other azoxyalkanes require heating to over 100 °C before N_2O extrusion sets in. In three cases side products due to further thermal reaction of the diene were observed. Compound **14** yields both cyclohexadiene and benzene. A control experiment revealed that the latter is a secondary product derived from oxidation of the former under the reaction conditions ($C_6H_5NO_2$, 131 °C). Azo *N*-oxides **15** and **16** deliver 1,3-cycloheptadiene and 1,3-cyclooctadiene, respectively, in addition to polymer upon pyrolysis. The latter arises from thermal degradation of the dienes at the reaction temperature ($C_6H_5NO_2$, 190 °C).

The Question of Concert. Although azo and azoxy derivatives of **2** and **31** thermolyze analogously from the point of view of product formation, the reactions occur with enormously different energy requirements. As we discuss in a subsequent section, unsaturated azoalkanes expel nitrogen with an activation energy of at least 24 kcal/mol less than the corresponding azo *N*-oxides. A meaningful comparison of the two systems requires knowing whether there is a changeover of mechanism for N_2 vs. N_2O loss when **2** is oxidized to **31.**

The unsymmetrical nature of the azo *N*-oxide moiety in **31** suggests the possibility for preferential C–N bond cleavage during N_2O loss. Formally three extreme candidates appear most likely as transients separating starting material and products: an unsymmetrical pericyclic transition state **32,** a zwitterionic intermediate with charge localized on the carbon fragment, **33a** and **33b,** and a diradical **33c.**

32

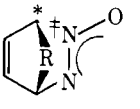

33a, (*, † = +, −)
b, (*, † = −, +)
c, (*, † = ·, ·)

A distinction among these possibilities can be made by considering the effects of bicyclic skeleton structure and solvent on the rate of thermal N_2O extrusion. Table II lists relative rates and $\Delta G^{\ddagger}$'s for a series of *N*-oxides. We regard compound **14** containing a single C=C bond the standard for comparison and begin with an analysis for intermediate **33a.** Replacement of the saturated ethane bridge by a cyclopropyl group (i.e., **17**) leads to a rate enhancement of 10^6 corresponding to a free-energy barrier drop of 11.3 kcal/mol at 132 °C. The analogous rate increase in the solvolytic generation of carbocations ranges

Table II. Thermolysis Rates for Unsaturated Azo *N*-Oxides

Compd	Solvent	$10^4 k$, s^{-1}	Rel rate (131.6 °C)	$\Delta G^{\ddagger}$, kcal/mol
17	CCl_4	2.5×10^4	1.3×10^6	23.2[a]
18	$C_6D_5NO_2$	3.0	150	30.5[a]
19		1.1	60	31.3[a]
14		2.0×10^{-2}	1.0	34.5[a]
15		9.8×10^{-4} [c]	4.9×10^{-2}	36.9[b]
16		5.2×10^{-4} [c]	2.6×10^{-2}	37.4[b]
21		4.1×10^{-6} [c,d]	2.0×10^{-4} <	>41.3[b,e]
20		4.1×10^{-6} [c,d]	2.0×10^{-4} <	>41.3[b,e]
22		4.1×10^{-6} [c,d]	2.0×10^{-4} <	>41.3[b,e]

[a] Determined at 131.6 °C. [b] Determined at 190 °C. [c] Rate calculated from the expression: $k_r = kT/h \times e^{-\Delta G^{\ddagger}/RT}$, with $\Delta G^{\ddagger}$ obtained at 190 °C and T = 131.6 °C. [d] Maximum value. [e] Minimum value.

from 100–500 [$\Delta\Delta G^{\ddagger}$ (20–60 °C) = 3.0–3.6 kcal/mol].[25] A particularly informative comparison arises by noting the result of exchanging the double bond in **14** for a cyclopropane ring (e.g., **22**). Cyclopropyl substitution is known to accelerate by 10–100 the formation of carbenium ions via solvolysis relative to the vinyl group [$\Delta\Delta G^{\ddagger}$ (20–30 °C) = 1.5–3.0 kcal/mol].[26] Table II shows, however, that cyclopropane **22** is at the very least 5000 times slower than olefin **14** [$\Delta\Delta G^{\ddagger}$ (132 °C) = 7 kcal/mol]. The same lower limit is exhibited by fusing a second cyclopropane onto the system (**21**) or by increasing the strain of the carbon backbone from that of a [2.2.2] to a [2.2.1] system (**22** → **20**, $\Delta E_{strain} \cong 5$ kcal/mol[27]). The latter is especially significant in view of the apparent thermal lability of *N*-oxide **13.** We conclude that the inverted cyclopropyl/vinyl response to decomposition of oxide **31** effectively rules out the intervention of intermediate **33a.**

The zwitterionic species **33b** places a negative charge on the hydrocarbon fragment. Rates of hydrogen exchange show that relative to RCH_2CH_2 the cyclopropyl moiety enhances the rate of formation of an adjacent carbanion by the diminutive factor of 2.4–11 [$\Delta\Delta G^{\ddagger}$ (43 and 160 °C) = 0.5–1.5 kcal/mol].[28] The $k_{17}/k_{14} = 10^6$ ratio would seem to exclude **33b** from consideration.

Finally we recall that since the unsubstituted cyclopropyl group increases the rate of incipient radical formation relative to CH_3 or i-C_3H_7 by a quantity of 10–30 [$\Delta\Delta G^{\ddagger}$ (95–135 °C) = 0.5–3.0 kcal/mol],[29] a diradical intermediate such as **33c** appears unlikely. Independent support for this supposition is derived from the thermal decomposition of the bicyclic azo *N*-oxide **34.** The latter disappears in a clean first-order reaction

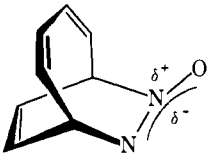

34

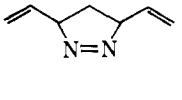

35

70 times faster than oxide **14** at 132 °C ($\Delta G^{\ddagger}$ = 31.1 kcal/mol; $C_6D_5NO_2$).[30] Pyrolysis of vinyl substituted 1-pyrazolines **35** has shown that a single vinyl group lowers the activation enthalpy by 8–10 kcal/mol,[4c] somewhat less than the delocalization energy of the allyl radical (12.6 kcal/mol).[31] The pentadienyl radical enjoys a resonance stabilization of ca. 20 kcal/mol[32] and might thus be expected to induce the lowering of a radical type transition state barrier by at least 15 kcal/mol. Were the radical mechanism operating in the azo *N*-oxide series, a significantly greater rate enhancement from **34** to **14** would be anticipated ($\gg\Delta\Delta G^{\ddagger}$ = 3.4 kcal/mol).

These arguments lead to the inference that unsaturated azo *N*-oxides expel N_2O by means of a concerted pathway symbolized by **32.** Kinetic measurements for the retrocycloaddition of compound **17** in different solvents support this contention.

Before proceeding with a discussion of the solvent studies one further mechanistic alternative for N_2O extrusion need be mentioned. A considerable number of cyclic azoalkanes have been implicated in the formation of diradical intermediates, e.g., **36.** The question naturally arises as to the possibility for an analogous intermediate **37** in the decomposition of unsaturated azo- and azoxyalkanes.

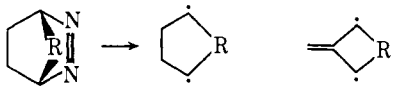

36 **40**

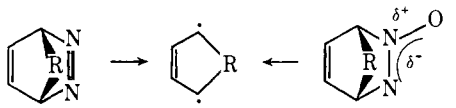

38 **37** **39**

Berson and his colleagues[12] have pointed out that saturated potential precursors of **36** routinely give ring closure products whereas unsaturated azo/azoxy precursors never do so. They speculated that **37** is most likely by-passed in favor of a concerted reaction. As written structure **37** can represent either a singlet or a triplet state. Its multiplicity and electronic structure will depend to a very high degree on geometry. For the saturated species **36** through-bond and through-space interaction of the electrons must be evaluted as a conformational problem. With R = $(CH_2)_n$, increasing n leads to an increasing diversity of interaction. All three geometric extremes, (0,0), (0,90), and (90,90)[4a,33] are then candidates for consideration. The existence of a double bond in **37,** however, requires that the unsaturated carbons and those bearing the electrons be in the same plane. Conformational flexibility is limited to the local structure at the radical sites. Even if the latter are nonplanar, the barrier to inversion is likely to be very low[34] providing a natural π channel for interaction of the electrons situated 1,4. The geometric factors are particularly favorable for cyclic species where R is a short chain of atoms. For cases of this kind, represented by most of the substances treated in the present investigation, the ground-state molecular wave function for **37** is essentially that for the corresponding cyclic diene. In valence bond language this means that **37** is simply a resonance structure of the latter. Thus from an operational point of view, so long as the azo and azoxy precursors contain unsaturation as shown for **38** and **39,** the diradical character symbolized by **37** need not be regarded as an entity separate from the product diene.

An interesting contrast is provided by the trimethylenemethane species **40,** isoelectronic with **37** but containing the C=C double bond cross-conjugated with the radical centers. Symmetry properties resulting from the near-equivalence of carbons 1–3 causes **40** to exist as a ground-state triplet.[5b,35]

Effect of Solvents on the Retrocycloaddition Rate. At 54 °C the rate of decomposition of azo *N*-oxide **17** decreases slightly

Table III. The Effect of Solvent on the Fragmentation of Azo *N*-Oxide **17**

Solvent	E_1 value	δ	$(\epsilon-1)/(2\epsilon+1)$	$10^4 k$, s^{-1} [a]	Rel rate	$\Delta G^{\ddagger}$ [a]	$\Delta H^{\ddagger}$ [b,c]	$\Delta S^{\ddagger}$ [b,c]
n-Hexane	30.9	7.3	0.188	14.0 ± 0.2	5.4	23.5		
CCl_4	32.5	8.6	0.225	11.5 ± 0.4	4.4	23.6	25.7 ± 0.3	6.2 ± 1.0
Dioxane	36.0	9.8	0.224	5.6 ± 0.06	2.2	24.1	24.4 ± 0.6	0.9 ± 1.9
EtOAc	38.1	8.9	0.385	5.2 ± 0.3	2.0	24.1		
DMF	43.8	11.8	0.480	3.0 ± 0.05	1.2	24.4		
CH_3CN	46.0	11.7	0.480	2.7 ± 0.2	1.0	24.5	26.5 ± 0.6	5.9 ± 2.0
EtOH, abs	51.9	12.7	0.470	2.6 ± 0.03	1.0	24.5	23.2 ± 0.5	−4.2 ± 1.6

[a] Determined at 54.0 ± 0.1 °C.[64] [b] At 25 °C. [c] Standard deviation from least-squares analysis.

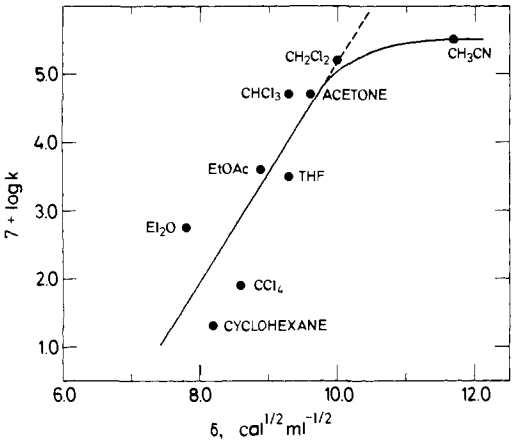

Figure 1. Log k for the cycloaddition of TCNE to anethole at 25 °C in various solvents plotted against the solvent parameter δ. Rate constants taken from ref 36.

with increasing solvent polarity (Table III), but is by and large insensitive to solvent structure. Zwitterionic intermediates **33a** and **33b** are immediately ruled out by comparison with a reaction for which the presence of similar species (**42**) has been

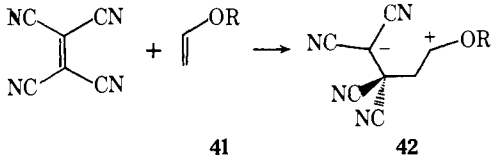

41 **42**

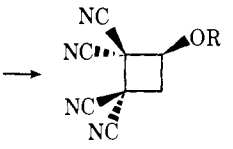

demonstrated. Steiner and Huisgen report that the rate of second-order cycloaddition of TCNE and enol ethers (**41**) increases by a factor 2600–29 000 when the solvent is changed from cyclohexane to acetonitrile.[36] Several lines of evidence implicate the 1,4-dipole **42** as an intermediate. For *N*-oxide **17** a solvent switch from *n*-hexane to CH_3CN causes a 0.19-fold reduction in rate.

Furthermore a plot of log k vs. E_T for the TCNE/**41** combination yields a good straight line as expected for reactions which involve a large change in polarity between the ground and transition states. On the contrary a plot of log k vs. δ, the solvent parameter which gives an experimental correlation for presumed one-step cycloaddition reactions,[37] leads to an apparent nonlinear relationship although CH_3CN was the only highly polar solvent investigated (cf. Figure 1). The analogous graphs for the N_2O extrusion of **17** (Figure 2) show the inverse relationship underscoring our conclusion by default in the previous section that N_2O loss is a concerted process.

It might be argued that the appearance of an E_T plateau in polar solvents signals a change in mechanism for the breakdown of **17**. Although this point will be considered in more detail in our discussion of activation parameters below, were a changeover operating, a similar plateau in the δ plot would likewise be anticipated. Consider, for example, the isomerization of bromocyclooctatetraene (**43**) to *trans*-bromostyrene.

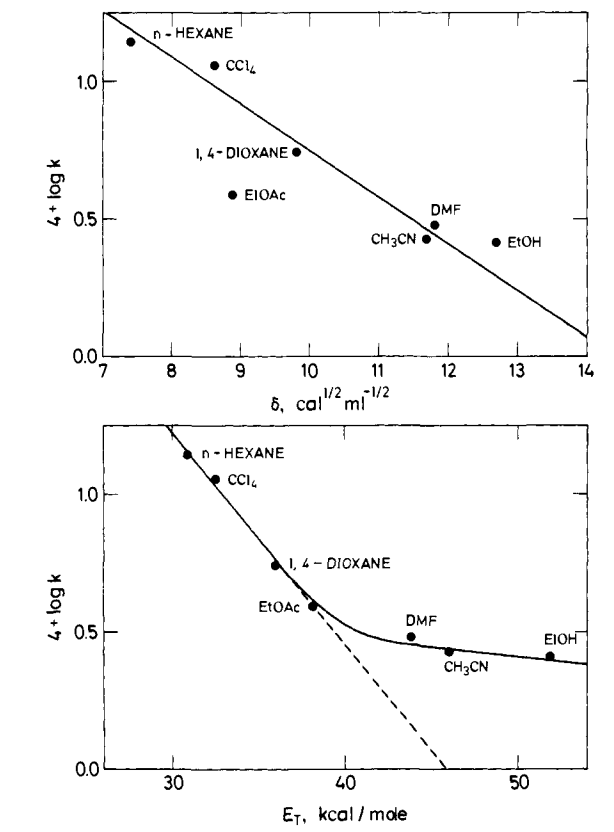

Figure 2. Log k for the cycloreversion of azo *N*-oxide **17** in various solvents at 54.0 °C plotted against the solvent parameters E_T and δ.

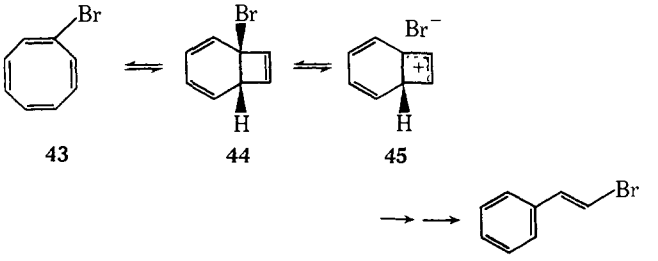

43 **44** **45**

The transformation takes place via the cationic intermediate **45** and likewise displays the E_T plateau in polar solvents.[38] This behavior was demonstrated to result from a shift of the rate-determining step from the ionization of bicycle **44** to the pericyclic valence isomerization of bromocyclooctatetraene. A graph of the corresponding isomerization rates for **43** vs. the solvent parameter δ also leads to a plateau (Figure 3)

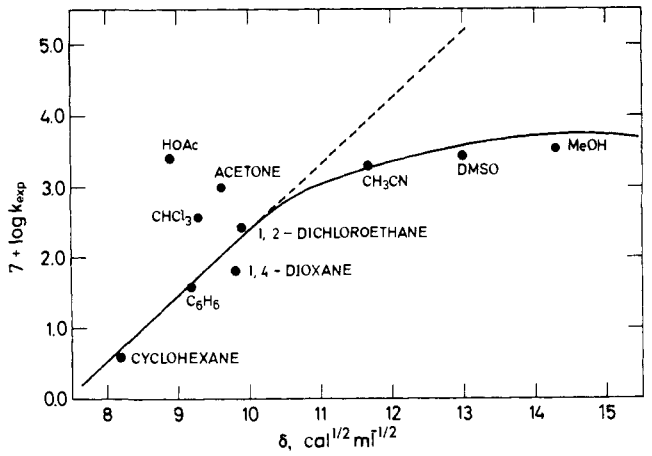

Figure 3. Log k for the isomerization of bromocyclooctatetraene to *trans*-bromostyrene at 79.5 °C in various solvents plotted against the solvent parameter δ. Rate constants taken from ref 38.

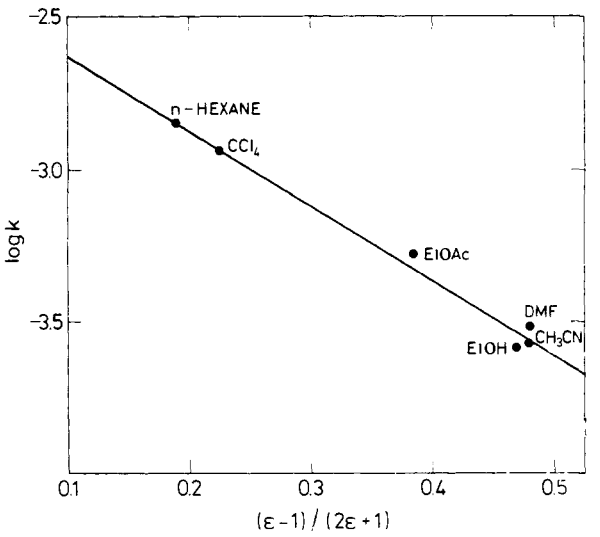

Figure 4. Log k for the cycloreversion of azo N-oxide **17** in various solvents at 54.0 °C plotted against the dielectric constant factor $(\epsilon - 1)/(2\epsilon + 1)$.

suggesting that the linear δ relationship for **17** (Figure 2) reflects the absence of ionic intermediates.

An additional mechanistic criterium derivable from solvent effects at a constant temperature is the change in substrate dipole moment as it moves from the ground state to the transition state. An approximate transition state dipole, $\mu_{\pm}$, can be calculated from Laidler and Eyring's extension[39] of Kirkwood's electrostatic model[40] for the rate constant dependence of the combination of two spherical dipolar molecules. The analogous expression for the fragmentation of a polar species into its parts is given by eq 1. The dielectric constant ratio $[(\epsilon - 1)/(2\epsilon + 1)]$ is plotted against log k at a specific temperature to provide the slope, m, of (1). Manipulation of this quantity leads to $\mu_{\pm}$ as in (2) in terms of m, the ground-state dipole moment (μ), the molecular volume considered as an idealized sphere $[V(r)]$, the transition state volume $[V_{\pm}(r_{\pm})]$, Boltzmann's constant (k_B), and the absolute temperature used to obtain m.

$$\ln k = \ln k_0 - \frac{1}{k_B T}\left(\frac{\mu^2}{r^3} - \frac{\mu_{\pm}^2}{r_{\pm}^3}\right)\left(\frac{\epsilon - 1}{2\epsilon + 1}\right) \quad (1)$$

$$\mu_{\pm} = \left[r_{\pm}^3\left(\frac{\mu^2}{r^3} + 2.303(m)(k_B)T\right)\right]^{1/2} \quad (2)$$

The dipole moment of azo N-oxide **17** is 4.77 D (C_6H_6, 20 °C).[41] The molecular volume is taken as 338 Å^3 (r = 4.3 Å) based on the known structures of **46** and **47** and standard bond

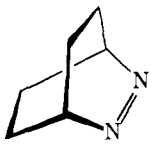

46

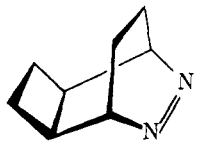

47

lengths and bond angles for the cyclopropane ring and the NO bond (see Experimental Section). An estimate of the transition state volume is obtained from the potential surface calculations described in a subsequent section ($V_{\pm}$ = 409 Å^3; $r_{\pm}$ = 4.6 Å). The slope of (1) at 54 °C is derived from the straight line of Figure 4 (r = 0.991) and found to be −2.43. These values lead to a minimum transition state dipole of $\mu_{\pm} \geq 1.7$ D.[42] Thus the transition state for N_2O extrusion in **17** is no less than one-third as polar as the N-oxide ground state in accord with synchronous cleavage of both C–N bonds. By comparison, the corresponding dipole moment increase for the transition state enol ether **41** and zwitterion **42** is estimated to be 700–900% that of the ground state (i.e., 1–2 to 10–14 D[36]).

Activation Parameters and Entropy Control. Deeper perception into the mechanism and driving force for azo N-oxide decomposition is afforded by evaluation of the enthalpy and entropy of activation as a function of solvent (Table III). As the solvent polarity increases from CCl_4 to absolute EtOH, the small overall rate decrease is reflected by an increase in $\Delta G^{\pm}$ of 1.0 kcal/mol. By contrast, $\Delta H^{\pm}$ shows opposite behavior and falls by 2.5 kcal/mol. Acetonitrile, an apolar diprotic solvent, is exceptional. The near rate constancy is a result of a compensating decrease in $\Delta S^{\pm}$. Table IV illustrates the dissection of these effects by listing the rate acceleration at constant $\Delta S^{\pm}$ and constant $\Delta H^{\pm}$, respectively. The clear-cut rate decrease with decreasing solvent polarity strongly suggests that N_2O elimination is entropy controlled.

Table IV. Rate Acceleration of the Decomposition of Azo N-Oxide **17** at Constant $\Delta S^{\pm}$ and Constant $\Delta H^{\pm}$

Solvent	$\Delta H^{\pm}$, kcal/mol	k_{rel}[a]	$\Delta S^{\pm}$, eu	k_{rel}[b]
CH_3CN	26.5	1.0	5.9	161
CCl_4	25.7	3.9	6.2	188
Dioxane	24.4	34.6	0.9	13
EtOH, abs	23.2	262.0	−4.2	1

[a] Calculated from the expression $k_1/k_2 = e^{(\Delta H_1^{\pm} - \Delta H_2^{\pm})/RT}$. [b] Calculated from the expression $k_1/k_2 = e^{(\Delta S_1^{\pm} - \Delta S_2^{\pm})/R}$.

Before discussing this point further, it is necessary to determine whether the inverse $\Delta H^{\pm}/\Delta S^{\pm}$ behavior is a genuine case of the well-known isokinetic relationship. Petersen, Markgraf, and Ross have argued that many reported cases of a linear correlation between $\Delta H^{\pm}$ and $\Delta S^{\pm}$ are in fact within experimental error.[43] They suggest that the range of $\Delta H^{\pm}$ values must exceed twice the maximum possible error, i.e., $\Delta H^{\pm} > 2\delta$, in order for the entropy–enthalpy relationship to be valid. The procedure is to assign a value to α, the maximum possible fractional error in k_1, and to calculate δ by means of expression 3. T_1 and T_2 represent the temperature limits for which the Arrhenius plots are constructed.

$$\delta \text{ (for } \alpha \ll 1) = 2R\alpha\left(\frac{T_1 T_2}{T_1 - T_2}\right) \quad (3)$$

For rate constants in CCl_4 least-squares analysis of ten runs at five different temperatures gave an average correlation coefficient of 0.9996. Duplicate runs yielded an average deviation of 2.4%. If α is taken as twice this value (0.048), δ is calculated to be 0.81 and 2δ = 1.6 kcal/mol. Since the range

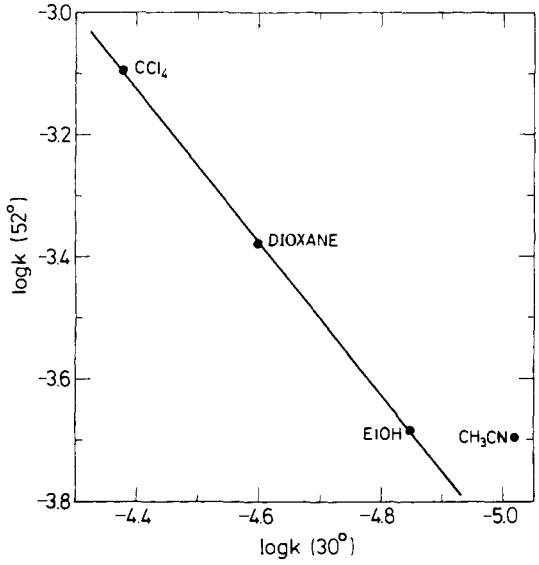

Figure 5. Isokinetic plot [log k(30 °C) vs. log k(52 °C)] for the decompostion of azo N-oxide **17** as a function of solvent.

of $\Delta H^{\ddagger}$ (excluding CH_3CN) is 2.5 kcal/mol, we regard the relation between $\Delta H^{\ddagger}$ and $\Delta S^{\ddagger}$ as a meaningful one.

A plot of $\Delta H^{\ddagger}$ vs. $\Delta S^{\ddagger}$ (25 °C) for CCl_4, dioxane, and absolute EtOH gives a straight line (r = 0.9999). However, in accord with Exner's suggestion[44] that a log-log plot is statistically superior for evaluating the data, the isokinetic temperature, β = −32.9 °C, is obtained from the slope (b) of the plot of Figure 5 and relation 4.

$$\beta = \frac{T_1 T_2 (1 - b)}{T_1 - bT_2} \qquad (4)$$

Since β is 63–88 °C below the temperature of measurement, it is permissible to conclude that in the three solvents which give an excellent straight line (r = 0.9999; with CH_3CN, r = 0.9690) the mechanism of N_2O loss is constant and, as deduced above, concerted. The fact that the isokinetic temperature lies below the average temperature of measurement signifies that the rate of reaction is being governed by $\Delta S^{\ddagger}$,[45] the entropy of activation. This result is another formulation of that implied by Table IV.

Comparison of medium effects on the decomposition of **17** and the retrocycloaddition of N_2 from the cyclopropyl azoalkane **48** is instructive. The data for the latter reaction show a

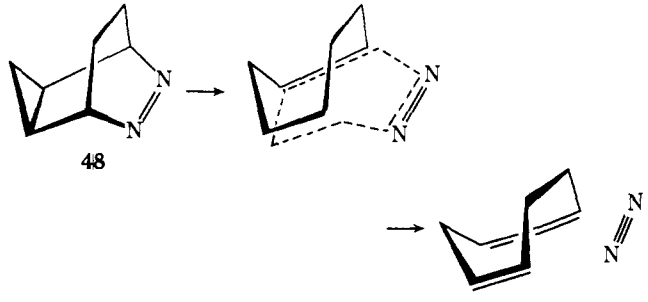

48

slight increase in rate corresponding to $\Delta\Delta G^{\ddagger}$ (25 °C) = 1.6 kcal/mol as the solvent ranges from isooctane to 96% etOH.[46] Superficially the extrusion of N_2 and N_2O from similar substrates (**48** and **17**, respectively) involves very similar energy requirements as a function of the reaction medium. A breakdown of the azo free energy of activation into its $\Delta H^{\ddagger}$ and $\Delta S^{\ddagger}$ components, however, reveals another pattern.[46] The azo decomposition is virtually insensitive to solvent polarity as expected for a symmetrical, concerted process. Although both $\Delta H^{\ddagger}$ and $\Delta S^{\ddagger}$ evidence ranges of 1.4 kcal/mol and 1.4 eu,

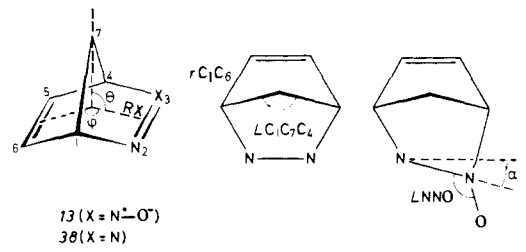

Figure 6. Optimized potential surface parameters for the CNDO/B[59] calculated heterofragmentation of azo **38** and azo N-oxide **13**. RX is the reaction coordinate.

respectively, the differences must be attributed to experimental error. As described above, N-oxide **17** shows a statistically significant spread in the activation parameters. The variations are small. Nevertheless, by comparison with the analogous quantities for azo **48**, they are consistent with synchronous cleavage of the C–N bonds, but with homolysis of the C–N(O) bond running ahead of that for the C–N bond. Similar moderate solvent effects have been observed for the unsymmetrical pericyclic transition states associated with 1,3-dipolar cycloaddition.[47]

Decomposition Mechanism for Unsaturated Azo *N*-Oxides in General. All of the above comments concerning the mechanism of N-oxide thermolysis apply strictly only to the labile derivative **17**. The greater energy requirements for N_2O expulsion of other members (Table II) have prevented a similar solvent study. Nevertheless we postulate that the clean release of N_2O for these species is likewise concerted. Several considerations support this contention, the first of which is the rate variation in response to structural modification. Two N-oxide series are of interest in this connection. The first concerns the relative rates for **22, 14,** and **17** as compared with the pericyclic retrocycloaddition of azoalkanes **48** and **49**.[48] The effect of cyclopropane vs. alkene substitution on extrusion rates evidences a close parallel for the two compound types (Scheme II).

The second series is **13–16.** Enlargement of the saturated bridge causes a drastic reduction in rate. Molecular models show quite clearly that the ground-state C=C p-orbital components are favorably disposed for overlap with the developing bridghead p orbitals in the transition state for the [2.2.1] system **13.** Increasing the angles around the bridgehead by homologation diminishes the bonding interaction by rotating the orbitals away from one another. A possible ground-state experimental measure of this effect is obtained from the photoelectron spectra of the bicyclic hydrocarbon dienes corresponding to N-oxide structures **13–16**.[49] The magnitude of the π–π splitting has been associated with the dihedral angle ϕ (cf. Figure 6) between the planes of the double bonds. For norbornadiene and bicyclo[2.2.2]octa-2,5-diene, ϕ = 116[50] and 123°,[51] respectively. The angle increases to 131 and 137° for the [3.2.2] and [4.2.2] bicycles. Thus for simultaneous cleavage of the C–N bonds, a qualitative rate gradation in the same order as the experimental one is anticipated. Unfortunately the stereoelectronic interpretation is not an unambigous one since strain release alone can conceivably account for the kinetic relationships.

Another indirect indicator of the operation of concert is the homogeneity of the products from N-oxide thermolysis. In all cases where a reaction is observed it proceeds cleanly to diene and N_2O. As pointed out above, the single exceptions arise from **14, 15,** and **16,** the product dienes of which lead to secondary products at the reaction temperature. Analogous azo decompositions which have been reported to pass through radical intermediates, e.g., **47,** likewise deliver product mixtures.[4a,b,52,53] Concerted cycloreversion of nitrogen from

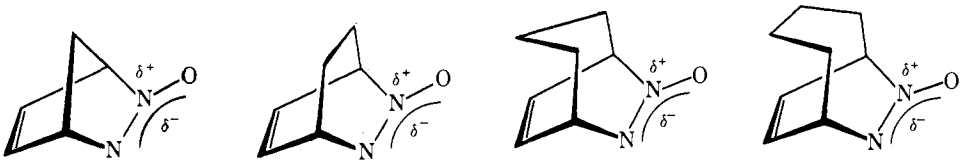

	13	14	15	16
k_{rel} (131.6 °C)	>>38	38	1.9	1.0

Scheme II

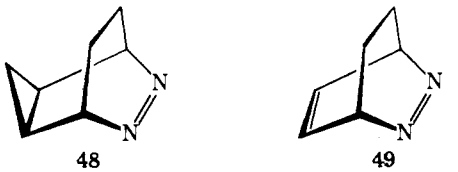

	48	49
k_{rel} (25.0 °C)	1	$> 3 \times 10^6$
k_{rel} (131.6 °C)	1	$> 6 \times 10^4$

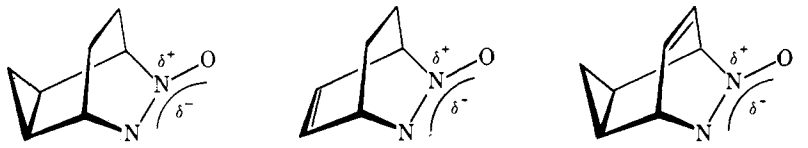

	22	14	17
k_{rel} (131.6 °C)	1<<	5.0×10^3	6.5×10^9

2 generally fulfills three mechanistic criteria: (1) high rates relative to saturated models, (2) the absence of ring closure products, and (3) product formation with high stereospecificity.[12] In the present investigation the bicyclic nature of the substrates prevent derivation of information concerning the latter. However, the general pattern of relative N_2O extrusion rates is entirely consistent with criterium 1, while the product simplicity of degraded *N*-oxides appears to reflect the operation of (2).

Participation of Four-Membered Rings in the Cycloreversion Reaction. Thermolysis of azo *N*-oxides **18** and **19** cleanly yields cyclooctatetraene and the 1,3,5-cyclooctatriene/bicyclo[4.2.0]-2,4-octadiene equilibrium mixture, respectively. Relative decomposition rates along the series **14, 19,** and **18** are 1:60:150 (131.6 °C, cf. Table II). The differences are small, but they invite speculation.

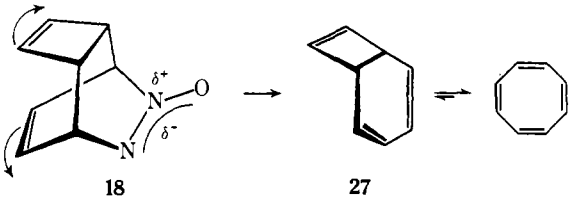

18 **27**

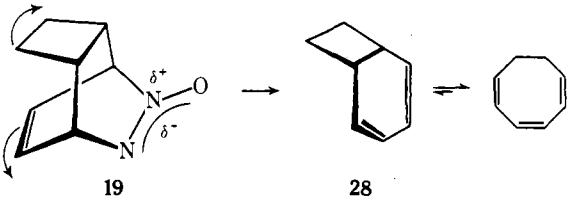

19 **28**

If it is assumed that the reactions are concerted, two sources for the rate increase of **18** and **19** over **14** are conceivable. The first arises from possible ground-state steric repulsion between the four-membered rings and the C=C bridge relaxed in the transition state (as indicated by the arrows). The bicycles **27** and **28** might then be the primary reaction products. As demonstrated above, the bicyclic hydrocarbons are, in fact, released from the corresponding azo compounds **29** and **30.** At the temperature of the *N*-oxide pyrolysis (131.6 °C), equilibrium between the mono- and bicyclic carbon species is established immediately so that the observed preponderance of the monocycles provides no insight into the nature of the primary products.[54]

X-ray analysis of the fully saturated azobicycle **47** reveals expanded bridghead angles reflecting a steric interaction between the cyclobutane ring and the CH_2–CH_2 bridge.[55] Furthermore both azo derivatives **46** and **47** have been shown to split out nitrogen via radical intermediates with a rate ratio of $k(47)/k(46)$ (131.6 °C) $\cong$ 2500.[9a,53] Molecular crowding of this type would therefore seem to be translatable into a rate enhancement. Were the reactions of **18** and **19** to proceed first to bicycles **27** and **28,** respectively, the moderate rate increases of N_2O loss over that for **14** are understandable. It is not at all obvious, however, that cyclobutene **18** would be expected to thermolyze 2.5 times as fast as the cyclobutane **19.** One case where steric effects do not seem to play a dominant role in a concerted cycloreversion concerns the relative rates of **50** and **51.**[9b] The compounds eliminate nitrogen with identical rates even though H–H repulsion at C-3 and C-8 in **50** might have resulted in acceleration.

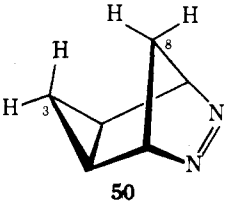

50

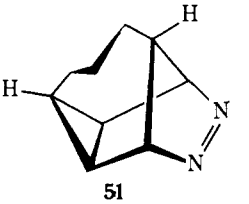

51

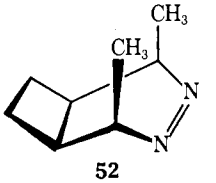

52

Consequently we prefer another rationalization which interprets the rate data as mirroring synchronous N_2O loss with simultaneous ring opening of the four-membered rings. Over and above the driving force provided by the ethylene bridges of **18** and **19,** a supplemental rate increment arises from strain release in the destruction of the small rings and from an electronic impulse exerted at the transition state by the incipient

Table V. CNDO/B Optimized Parameters for the N_2 and N_2O Extrusion Reactions of Azo **38** and Azoxy **13**, Respectively (cf. Figure 6 for Parameter Definition)[a,b]

RX, Å		rC_1C_6, Å		$\angle C_1C_7C_4$		θ		ϕ			
Azo	Azoxy	Azo	Azoxy	Azo	Azoxy	Azo	Azoxy	Azo	Azoxy	∠NNO	α
1.313	1.318	1.560	1.578	85.5	90.3	122.2	122.3	111.6	110.9	126.9	−0.2
1.5		1.545		94.5		116.0	118.6	108.5	107.0	126.7	+6.2
1.7		1.505		97.0		108.3	111.4	104.3	103.5	128.7	+12.3
1.9		1.454		100.5		99.7	105.9	99.1	101.1	145.8	+13.3
2.1		1.434		104.4		97.3	98.0	96.9	96.6	158.1	+9.9
2.4		1.424		107.2		92.0	92.7	93.7	94.2	168.5	+2.4
3.0		1.421		108.4		87.1	86.5	93.7	94.7	179.1	−2.0

[a] All angles in degrees. [b] Other points with RX = 2.0, 2.2, 2.3, 2.5, 3.5, and 4.0 Å follow the tabulated trends.

cyclobutane/cyclobutene C–C bonds. Berson, Petrillo, and Bickart have elegantly demonstrated that the cyclobutane rings of **52** and its methyl epimer evidence such behavior attended by small rate enhancements.[11] For example azo **52** decomposes only about five times the rate of tricycle **47.** Other cases have been reported.[56,57]

The participation of the four-membered rings in the N_2O extrusion is furthermore compatible with the rate ratio k(**18**)/k(**19**) (131.6 °C) = 2.5. Cyclobutene has recently been estimated to contain 3.7 kcal/mol more strain energy than cyclobutane.[58] Kinetic measurements for the ring opening of bicyclooctatriene **27** and bicyclooctadiene **28** to cyclooctatetraene and 1,3,5-cyclooctatriene, respectively, are qualitatively similar and lead to the ratio k(**27**)/k(**28**) (131.6 °C) = 561.[54] We conclude that **18** and **19** fragment by means of activated complexes symbolized by structures **53** and **54.** The divergence

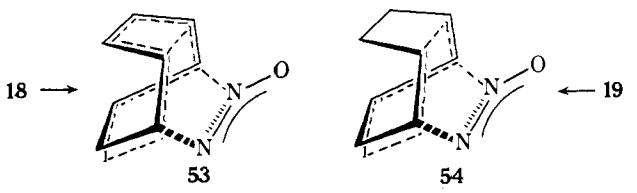

53 **54**

of behavior from azo compounds **29** and **30** results from the extreme thermal stability of *N*-oxides relative to the corresponding unsaturated azoalkanes. The higher temperatures necessary for thermal degradation are sufficient to promote the subsidiary bonding changes. For investigating subtle effects of weakly interacting substituents the stable azo *N*-oxides consequently stand as useful models for dihydro azo systems **2** in those cases where the latter may fragment by alternative pathways (e.g., **29** and **30**) or may be too reactive to observe directly.

Retrocycloaddition Pathway. CNDO/B Calculations. Both the effect of structure and solvent on the rates of N_2 and N_2O retrocycloaddition suggest a resemblance in the azo and azo *N*-oxide transition states. An attempt to obtain structural details for the cycloreversion has been made by computing the reaction hyperplane for the bicyclo[2.2.1] derivatives **13** and **38** (R = CH_2). Ground-state structures for the latter were derived by a complete CNDO/B[59] optimization of geometry as a function of total energy. The refined structural parameters are given in the Experimental Section. Figure 6 indicates how the potential energy surfaces for N_2 and N_2O extrusion have been defined.

The bridghead carbons C_1 and C_4 were held stationary while the fragment N–X was gradually separated, RX being employed as the reaction coordinate. Most of the bond lengths and bond angles found by optimization of the bicyclic ground states were transformed slowly into the values for cyclopentadiene, N_2, and N_2O. However, in order to obtain a realistic hypersurface, certain of the structural parameters were optimized likewise at each step of the computed reaction. For the azoalkane **38** (X = N, Figure 6) rC_1C_6, $\angle C_1C_7C_4$, and dihedral angles θ and ϕ were varied at each value of RX. A plane of symmetry containing C_7 and bisecting the C_5C_6 and NN bonds was maintained throughout. There is no a priori reason for assuming C_s symmetry as has been pointed out by several groups.[60] At the transition state several unsymmetrical orientations of N_2 and C_5H_6 were calculated. Although the energy maximum appears to be best represented by a relatively shallow saddle point, the lowest total energy is predicted to be the symmetrical complex. For the *N*-oxide **13** (X = N^+–O^-, Figure 6), optimized rC_1C_6 and $\angle C_1C_7C_4$ azo values were carried over unchanged, but θ, ϕ, α, and ∠NNO angles were relaxed at each RX distance. The results are given in Table V.

Seen from an overall geometric viewpoint the symmetrical cycloreversion of azo **38** is unexceptional and in complete accord with a concerted process insensitive to reaction medium.[46] The *N*-oxide **13** decomposition is predicted to proceed in a single step but with unequal rates of cleavage of the C–N bonds. This is reflected by the variation of angle α (Figure 6) from −0.2° to a maximum of 13°, then back to zero as the fragments pass to infinite separation. The computed transition state is accurately depicted by structure **32** and is in remarkable agreement with our deductions made from the response of $\Delta H^{\ddagger}$ and $\Delta S^{\ddagger}$ to solvents of widely differing polarity. The calculated reduction in dipole moment ($\Delta\mu_{calcd}$ = 3.8 D) from ground state to transition state likewise reflects the change in charge distribution obtained by application of Laidler and Eyring's reactivity model as expressed by eq 1 ($\Delta\mu_{exp} = \mu$(**17**) $- \mu_{\ddagger} \leq 3.1$ D).

***k*(azo)/*k*(azoxy) Ratio.** We have previously described the energetic consequences of storing unsaturated azoalkanes such as **2** in the form of their *N*-oxides **31.** The fleeting intermediacy of the former is altered in every case so that the latter exist as shelf stable substances. A comparison of the lability of azo bicycle **49** with that of *N*-oxide **14** indicated that for the heteroextrusion reaction, k(azo)/k(azoxy) ≥ 10^{17} (25 °C) corresponding to a ΔE_a (azo − azoxy) ≥ 24 kcal/mol.[13]

One of the motivations for the calculations described in the previous section was to try to reproduce the experimental energy difference in order to probe its origins. The results have been disappointing. Both azo **38** and azoxy **13** decompositions are calculated to be highly endothermic. In itself this does not invalidate the calculated total energy changes since the spontaneity of the retrocycloadditions is possibly governed by the increase in entropy associated with fragmentation into two particles. Since, however, ΔS and $\Delta S^{\ddagger}$ for both N_2 and N_2O loss can be expected to be at least of the same order of magnitude, activation enthalpies most likely control the overall energetic differences of the reactions. The calculated differences $\Delta\Delta E$(azo − azoxy) for the quantities ΔE(ground state − ground state) and ΔE(ground state − transition state)

amount to only 2–4 kcal/mol, hardly enough to account for the observed rate ratios.

There seem to be two major deficiencies in the calculated total energy values. On the one hand semiempirical parameterizations of the CNDO/INDO variety are known to underestimate strain energies seriously.[61] For the highly strained [2.2.1] bicycles **13** and **34** (strain energy ≥ 30 kcal/mol[62]), this factor is probably constant. Secondly while CNDO/B was parameterized on N_2, it overestimates the bonding energy of N_2O by 23 kcal/mol.[59] Thus while the potential surface calculations suggest a nearly identical shape for the one-dimensional azo and azo *N*-oxide hypersurfaces, it is clear that they must be skewed on the product side by at least 20 kcal/mol.

A satisfying understanding of the magnitude of ΔE_a(azo − azoxy) awaits a reliable theoretical evaluation of the cycloelimination pathways and calorimetric measurements of the respective ground-state energy differences.

Experimental Section

General. Microanalyses were performed by the Micronanalytical Laboratory, Kemisk Laboratorium II, H. C. Ørsted Institute, the University of Copenhagen. Melting points were determined on a Reichert melting point microscope and are uncorrected. Infrared spectra were recorded with a Perkin-Elmer Model 337 grating infrared spectrophotometer. Untraviolet spectra were obtained with a Unicam SP 800 A or a Unicam 1800 ultraviolet spectrophotometer. The proton magnetic resonance spectra were traced on a Varian A-60A instrument with approximately 10% solutions at ca. 40 °C with tetramethylsilane (Me_4Si) as internal standard. GLC analyses were accomplished with a Perkin-Elmer F 11 gas chromatograph or a Pye Unicam 104 chromatograph. Both were equipped with a flame ionization detector. Except where noted, solvents were reagent grade and used as received.

Diazabasketane Adduct. 4-Methyl-2,4,6-triazahexacyclo[5.4.2.0^{2,6}.0^{8,11}.0^{9,13}.0^{10,12}]tridecane-3,5-dione (7). A solution of urazole diene **6**[14] (7.50 g, 34.5 mm) in acetone (700 ml) was degassed by purging with nitrogen, magnetically stirred, and irradiated through Pyrex (Phillips 400-W lamp) for 24 h. The solvent was evaporated to dryness and the residual solid (8.1 g) column chromatographed (silica gel, ether) to give a white solid (5.7 g). Recrystallization (ethyl acetate) afforded colorless crystals, **7**, (5.20 g, 23.9 mm, 69%), mp 119–120 °C.

Anal. Calcd for $C_{17}H_{11}N_3O_2$: C, 60.8; H, 5.1; N, 19.4. Found: C, 60.9; H, 5.0; N, 19.6.

^{1}H NMR τ ($CDCl_3$/Me_4Si) 5.00 (2 H, septet), 6.32 (4 H, pentet), 6.67 (2 H, quartet), 6.90 (3 H, s); IR ν_{max} ($CHCl_3$) 1760 (m), 1695 (s), 1470 (m), 1400 (m), 1220 (m), 945 (m) cm^{-1}.

Rearrangement of Diazabasketene 7 to Diazasnoutene 8. A solution of the diazabasketene derivative **7** (2.17 g, 10.0 mm) and powdered silver nitrate (27.6 g, 150 mm) in methanol–water (4:1, 400 ml) was heated at reflux for 72 h in the dark. The cooled solution was treated with water (700 ml) and extracted with methylene chloride (6 × 100 ml). The combined extracts were washed with water (2 × 100 ml), dried over $CaCl_2$, and evaporated to dryness giving a white solid (1.85 g, 8.5 mm, 85%), the NMR of which was superimposable with the analytical sample. Recrystallization (96% EtOH) provided white needles, **8** (1.57 g, 7.2 mm, 72%), mp 226–228 °C.

Anal. Calcd for $C_{11}H_{11}N_3O_2$: C, 60.8; H, 5.1; N, 19.4. Found: C, 60.7; H, 5.3; N, 19.4.

^{1}H NMR τ ($CDCl_3$/Me_4Si) 4.95 (2 H, pentet), 6.91 (3 H, s), 7.7–8.2 (6 H, m); IR ν_{max} ($CHCl_3$) 1770 (m), 1700 (s), 1470 (m), 1405 (m), 1220 (m), 975 (m), 810 (m) cm^{-1}.

4-Methyl-2,4,6-triazaquadricyclo[5.4.2.0^{2,6}]tridec-12-ene-3,5-dione (9). A mixture of diene **6** (1.10 g, 5.0 mm) in ethyl acetate (125 ml) and 5% Pd/C (20 mg) was hydrogenated on an apparatus capable of quantitative measurement of hydrogen uptake. Hydrogen (120 ml) was absorbed within half an hour. The mixture was filtered through celite and the clear filtrate concentrated in vacuo to give a white solid (1.05 g, 4.9 mm, 98%) which was shown to be 95% pure by NMR. Recrystallization (ether) afforded white cyrstals (870 mg, 4.0 mm, 80%), mp 120–121 °C.

Anal. Calcd for $C_{11}H_{13}N_2O_3$: C, 60.3; H, 6.0; N, 19.2. Found: C, 60.6; H, 6.2; N, 19.3.

^{1}H NMR τ ($CDCl_3$/Me_4Si) 3.42 (2 H, t), 5.18 (2 H, m), 6.8–7.2 (m), 7.01 (3 H, s), 7.6–8.7 (4 H, m); IR ν_{max} ($CHCl_3$) 1770 (m), 1700 (s), 1400 (m) cm^{-1}.

***exo*-Methyl-2,4,6,10,11-pentaazaquadricyclo[5.5.1.0^{2,6}.0^{8,12}]tridec-9-ene-3,5-dione (10).** To a solution of the cyclopentadiene adduct **4** (n = 1) (10.2 g, 56 mm) in absolute ether/absolute ethanol (3:2, 250 ml) was added a solution of freshly prepared diazomethane (from *p*-tolylsulfonylmethylnitrosoamide,[63] ca. 2.7 g, 64 mm) in absolute ether (400 ml). The reaction mixture was allowed to stand at 0–5 °C for 6 days. Excess diazomethane was destroyed by adding dilute acetic acid until nitrogen evolution ceased. Ether and ethanol were removed by evaporation. The residue was made slightly basic with sodium bicarbonate and extracted with chloroform (2 × 75 ml). Removal of solvent from the combined extracts gave a brown oil. Soxhlet extraction with ether gave a light-yellow crystalline compound **10** (6.0 g, 31 mm, 56%), mp 98–105 °C. This material was used without further purification for the subsequent photolysis step to produce cyclopropane **11.**

^{1}H NMR τ ($CDCl_3$/Me_4Si) 4.7–5.7 (5 H, envelope), 6.96 (3 H, s), 7.5 (1 H, m), 8.60 (2 H, AB quartet with additional splitting); UV λ_{max} (MeOH) 225 (ϵ 3400), 314 nm (ϵ 405).

***exo*-4-Methyl-2,4,6-trizaquadricyclo[5.3.1.0^{2,6}.0^{8,10}]trideca-3,5-dione (11).** A degassed solution of pyrazoline **10** (4.00 g, 21.0 mm) in acetonitrile (500 ml, passed through a column of neutral aluminum oxide before use) was irradiated under nitrogen at 3500 Å for 2 days in a Rayonet photochemical reactor. Removal of solvent under reduced pressure afforded a brown oil which was clarified by chromatography on a preparative silica gel plate with ether. The resulting solid was recrystallized (ether) to yield colorless needles **11** (1.22 g, 7.4 mm, 36%), mp 114–115 °C.

Anal. Calcd for $C_9H_{11}N_3O_2$: C, 56.0; H, 5.7; N, 21.7. Found: C, 55.8; H, 5.9; N, 21.6.

^{1}H NMR τ ($CDCl_3$/Me_4Si) 5.38 (2 H, broad s), 6.95 (3 H, s), 8.2–8.7 (4 H, m), 9.3–9.7 (2 H, m); IR ν_{max} (KBr) 3080 (w), 3045 (w), 3010 (w), 2980 (w), 2945 (w) cm^{-1}. Starting material **10** was likewise isolated (550 mg, 14%).

Anthracene–MTAD Adduct 10. A solution of anthracene (3.14 g, 18.0 mm) in dry dioxane (50 ml) was mixed with a solution of 3-methyl-1,2,4-triazoline-3,5-dione (MTAD)[14] (2.82 g, 18.0 mm) in dry dioxane (50 ml). After 3 days at room temperature (stirred under N_2), the discharge of color was complete. Solvent evaporation produced a white solid; recrystallization (benzene) gave white crystals (3.60 g, 12 mm, 70%), mp 242–243 °C.

Anal. Calcd for $C_{19}H_{13}N_3O_2$: C, 70.1; H, 4.5; N, 14.4. Found: C, 70.0; H, 4.5; N, 14.4.

^{1}H NMR τ ($CDCl_3$/Me_4Si) 2.72 (8 H, m), 3.87 (2 H, s), 7.22 (3 H, s).

***cis*-Azoxyalkanes.** Both of the following represent the general procedures which utilize *N*-methylurazole adducts as precursors.

Method I. Cf. method B, ref 14. For variations in reaction time and temperature, see Chart I; for yields and physical data, Table I.

Method II. *exo*-6,7-Diazatricyclo[3.2.2.0^{2,4}]non-6,8-diene *N*-Oxide (17). A mixture of *N*-methyltriazoline dione adduct **5** (4.16 g, 20 mm), ethylene glycol (50 ml), and 35% hydrogen peroxide (130 ml) was treated with a solution of potassium hydroxide (85% KOH, 100 g, ca. 1520 mm; optimum KOH/adduct ratio: ca. 75/1) in distilled water (100 ml). The addition should be conducted in such a way that the temperature of the reaction mixture never exceeds 45 °C. This temperature was maintained for 130 min as 35% hydrogen peroxide (30 ml) was added dropwise continously to maintain an excess of oxidant. The cooled mixture (−20 °C) was extracted three times with *cold* chloroform (3 × 100 ml). Extracts were combined, dried over calcium chloride, then magnesium sulfate at −40 °C. Removal of solvent (−20 °C, 1 mm) produced a white solid (1.89 g, 14 mm, 70%). The NMR spectrum of the crude product showed starting material and azoxy compound **17** to be present in a ratio of 1:11. Double recrystallization from ether at −20 °C afforded white needles (1.35 g, 10 mm, 50%).

Azoxyalkanes **18**–**21** were prepared accordingly. All are crystalline solids and completely stable under 100 °C. Reaction workup at room temperature is therefore permissible. For variations in reaction time and temperature, see Chart I; for yields and physical data, Table I.

Hydrolytic Oxidation of MTAD Adduct 4 (n = 1). (a) A flask containing a solution of *N*-methyltriazolinedione adduct **4** (n = 1) (0.179 g, 1.0 mm), ethylene glycol (2.5 ml), and 35% hydrogen peroxide (6.5 ml) was attached to a dry ice trap, purged with nitrogen, and treated

Table VI.

Compd	Temp, °C	*N*-Oxide protons monitored, τ	10^4, s^{-1}	Correl coeff
14	131.6	3.46 (vinylic)	$(1.97 \pm 0.06) \times 10^{-2}$	0.996
19	131.6	4.64 (bridgehead)	1.10 ± 0.05	0.995
18	131.6	6.83 (cyclobutyl)	2.98 ± 0.17	0.992
15	190	3.62 (vinylic)	0.356 ± 0.012	0.998
16	190	5.08 (bridgehead)	0.211 ± 0.040	0.982

Chart I

	14	**15**	**16**	**18**	**19**	**20**	**21**
Method	I	I	I	II	II	II	II
Time (min)	60	60	90	150	100	40	90
Temp (deg)	80–95	80–95	80–95	45–55	50–55	65–80	70–80

with a solution of 5.0 g of potassium hydroxide in 5 ml of distilled water for 2 min at 30–40 °C. After 25 min at 35–40 °C the solution was cooled. Cyclopentadiene (28 mg, 0.42 mm, 42%) was collected and identified by NMR [τ ($CDCl_3$/Me_4Si) 3.48 (4 H), 7.04 (2 H)].

(b) A mixture of *N*-methyltriazolinedione adduct **4** (n = 1) (0.358 g, 2.0 mm), ethylene glycol (5 ml), and 35% hydrogen peroxide (13 ml) was treated with a solution of 10.0 g of potassium hydroxide in distilled water (10 ml) for 5 min at 30–40 °C. After 15 min at 35–40 °C the reaction mixture was cooled and extracted with cold methylene chloride (2 × 20 ml). The combined extracts were dried over calcium chloride and titrated with the cherry-red MTAD (0.224 M). After consumption of 1.9 ml (0.43 mm, 21%), the solvent was evaporated to produce a yellow solid (100 mg). The NMR spectrum was superimposable with that of adduct **4** (n = 1). Neutralization of the remaining aqueous phase with concentrated HCl, extraction with chloroform (2 × 20 ml), and drying of the combined extracts over $CaCl_2$ produced a solution which decolorized the cherry red solution of MTAD in methylene chloride. After consumption of 0.8 ml, solvent evaporation produced a solid (47 mg, 0.18 mm, 9%), the NMR of which was identical with that of **4** (n = 1).

Azoxy Deoxygenation with Si_2Cl_6, Room Temperature. *N*-oxides **14, 15,** and **17** (ca. 50 mg) were each dissolved in $CDCl_3$ (1% Me_4Si, ca. 0.5 ml) and treated with excess of Si_2Cl_6 (ca. 0.3 ml) in an NMR tube. The tube was shaken vigorously as a mildly exothermic reaction took place. Within 10 min all of the azoxyalkane had disappeared, and its spectrum was replaced by that of cyclohexadiene, cycloheptadiene, and cycloheptatriene, respectively. None of the intermediate spectra exhibited peaks other than those attributable to starting *N*-oxide and product diene.

Azoxy Deoxygenation with Si_2Cl_6, Low Temperature. The *N*-oxides (60–70 mg) were dissolved in $CDCl_3$ (1% Me_4Si, ca. 0.5 ml), placed in an NMR tube, cooled to −78 °C, and treated with an excess of Si_2Cl_6 (ca. 0.3 ml). The tube was agitated and transferred to an NMR probe (Varian A60-A) precooled to −40 °C. Spectra taken at this temperature were superimposable with those of the analytically pure azoxyalkanes. The probe was warmed at 10 °C intervals and a spectrum recorded at each step. In all cases the *N*-oxide absorption was gradually replaced only by that of the corresponding olefin. In none of the experiments was there evidence for an intermediate species.

a. [4.2.2] *N*-Oxide 16. At −30 °C 30–40% of **16** was converted after 1 h.

b. Cyclobutyl *N*-Oxide 19. No changes in the azoxy spectrum were observed up to 0 °C. At this temperature deoxygenation was complete within 30 min to give bicyclo[4.2.0]-2,4-octadiene (τ 4.31, 6.96, and 7.66).

c. Cyclobutenyl *N*-Oxide 18. The *N*-oxide spectrum remained uncontaminated up to −15 °C. At −10 °C a few percent of bicyclo[4.2.0]-2,4,7-octatriene appeared. Over a 1.5-h period at 0 °C the corresponding bands at τ 4.12, 4.30, and 6.65 slowly developed but were gradually overtaken by the cyclooctatetraene singlet at τ 4.25.

d. Snoutene *N*-Oxide 21. The spectrum of semibullvalene (τ 4.85, 5.76, and 6.97) began to appear after 2 h at −35 °C (few %). A slow increase of the temperature to −10 °C over 95 min produced ca. 15% of the hydrocarbon. During a final 60-min period, the temperature was raised to 40 °C during which time conversion to semibullvalene was complete.

Kinetic Measurements for the Fragmentation of Azo *N*-Oxide 17. All solvents were distilled and then passed through a basic aluminum oxide column before use. The reaction was followed with a Unicam SP-800 A/SP-820 ultraviolet spectrophotometer.

Solvent Dependence. Measurements were carried out at UV concentrations with recrystallized *N*-oxide **17** in a thermostated cell block of the spectrophotometer. (T = 54.0 ± 0.1 °C).[64] Automatic rescan of the solutions gave families of reproducible spectra. Each reaction was run in duplicate, followed to several half-lives and the absorbance monitored at 275 nm. Unimolecular rate constants were obtained by least-squares analysis of $\ln(A_{infinite} - A_t)$ vs. time. A correlation coefficient of 0.999 was routinely obtained. Final values (Table II) are the average of two runs. Isobestic points were observed for *n*-hexane at 249.6 nm, in dioxane at ca. 250 nm, in acetonitrile at 250.2 nm, and in absolute ethanol at 249.5 nm. For CCl_4 and ethyl acetate solvent cut-off prevented its observation.

The hydrocarbon product, cycloheptatriene, was established by GLC and NMR analyses by comparison with an authentic sample. Integration against Me_4Si as internal standard indicated that cycloheptatriene was produced in quantitative yield (>96%). No other products could be detected.

Temperature Dependence. Eyring activation parameters were obtained by scanning the retrocycloaddition as specified above at a minimum of five different temperatures. The temperature was measured directly in the cell by means of a finely graduated thermometer (ΔT = ±0.1 °C). A least-squares fit of ln k vs. $1/T$ (K) provided the values of $\Delta H^{\ddagger}$, $\Delta S^{\ddagger}$, and $\Delta G^{\ddagger}$ listed in Table III. Error limits correspond to the standard deviation.

Kinetic Measurements for the Fragmentation of Azoxyalkanes in Deuterionitrobenzene. Each *N*-oxide (ca. 50 mg) was dissolved in degassed $C_6D_5NO_2$ (~500 μl) with a corresponding quantity of anisole (internal standard) and sealed in a thick-wall NMR tube. The samples were heated at 131.6 ± 0.2 or 190 ± 2 °C over several half-lives and periodically monitored at room temperature by integration (10×) of certain azoxy protons (cf. Table VI) against the methyl protons of anisole. Unimolecular rate constants were derived by least-squares analysis of ln(azoxy-integral/CH_3O-integral) vs. time.

Product identity was established by comparison of NMR spectra and GLC traces of the product solutions and authentic diene samples. Compounds **18** and **19** delivered quantitatively (>95%) cyclooctatetraene and the 1,3,5-cyclooctatriene/bicyclo[4.2.0]-2,4-octadiene equilibrium mixture, respectively. *N*-oxide **14** yielded a mixture of 1,3-cyclohexadiene and benzene. Bicycles **15** and **16** led to 1,3-cycloheptadiene and 1,3-cyclooctadiene, respectively, but NMR analysis indicated that both of the latter polymerize somewhat under the pyrolysis conditions (190 °C). For these five cases, no products other than those mentioned could be detected. Conditions and results are tabulated in Table VI.

For compounds **20, 21,** and **22,** the solutions maintained at 190 ± 2 °C were checked periodically by NMR integration of the bridgehead hydrogens against anisole-OCH_3. No decomposition was evident after 28 h. A similar negative result was obtained by GLC analysis using authentic diene controls.

Calculations. 1. CNDO. Retrocycloaddition of Azo 38 and Azo-*N*-Oxide 13 (cf. Figure 6). The ground-state geometries of these bicycles were fully optimized by the CNDO/B procedure:[59] **38/13**

(bond distances, Å; bond angles, deg) rNN = 1.203/1.221, rNC = 1.414/1.416, rC_1C_6 = 1.560/1.578, rC_1C_7 = 1.592/1.593, rC_5C_6 = 1.408/1.410, rCH = 1.089-1.101, rNO = 1.262, $\angle CNN$ = 111.8/111.7, $\angle C_1C_6C_5$ = 105.7/109.6, $\angle C_1C_7C_4$ = 90.0/90.8, $\angle NNO$ = 126.9, $\angle C_5C_6H$ = 129.9/130.6, $\angle HC_7H$ = 108.6/109.0. Table V lists optimized parameters for the N_2 and N_2O extrusion reactions. The energy maxima were computed to be at RX = 2.3 and 2.4 Å, respectively. For **38** at RX = 2.1, 2.3, and 2.5 Å, a number of unsymmetrical orientations of N_2 relative to the hydrocarbon backbone were calculated. Structures maintaining the C_1NNC_4 atoms in a common plane as well as twisted geometries were considered. In every case the total energy increased relative to the symmetrical species.

2. Transition State $\mu_\pm$ for Azo *N*-Oxide 17. For the purposes of obtaining r (eq 1 and 2), the following structural values were assigned to **17** based on the known geometries of various bicyclic azoalkanes[56] and cyclopropane: (bond distances, Å, bond angles, deg) rNN = 1.290, rNC = 1.497, rC_1C_7 = 1.539, rC_1C_8 = 1.521, rC_5C_7 = 1.553, rC_5C_6 = 1.521, rC_8C_9 = 1.338, rNO = 1.290, $\angle CNN$ = 114.9, $\angle C_1C_7C_5$ = 108.3, $\angle C_1C_8C_9$ = 112.3, $\angle NNO$ = 120.0, dihedral angle (cyclopropane ring/$C_1C_4C_5C_7$ plane) = 116.1. Consideration of the nuclear coodinates alone permits the resulting structure to reside within a sphere of radius r = 2.56 Å. With the addition of van der Waal's radii of 1.5 and 2.4 Å for H and O^-, respectively, the sphere expands to one with r = 4.32 Å. The transition state species was simulated by taking the N_2O moiety values from Table VI (RX = 2.4 Å) and deforming the hydrocarbon backbone accordingly. The required $r_\pm$ = 2.85 (nuclear coordinates) and 4.61 Å (van der Waals radii). The slope of the log k vs. $(\epsilon - 1)/(2\epsilon + 1)$ plot is −2.43 (correlation coefficient 0.991) obtained by dropping the dioxane value of Table III. Previous work has shown this solvent not to conform to the correlation.[37b] The transition state dipole moments from (1) are $\mu_\pm$ = 5.05 D (nuclear coordinates) and 1.70 D (van der Waal's radii).

Acknowledgment. We are grateful to the Danish Natural Science Research Council (Grant no. 911-5153) for their generous support of the work.

References and Notes

(1) *cis*-Azoxyalkanes. 8. For Part 7, see J. C. Bünzli, H. Olsen, and J. P. Snyder, *J. Org. Chem.*, in press; for part 6, see ref. 14b.
(2) Cf. R. B. Woodward and R. Hoffmann, *Angew. Chem., Int. Ed. Engl.*, **8**, 781 (1969), for numerous examples of cheletropic reactions; W. L. Mock, *J. Am. Chem. Soc.*, **97**, 3666 (1975); **97**, 3673 (1975).
(3) R. Criegee and A. Rimmelin, *Chem. Ber.*, **90**, 414 (1957); R. M. Moriarity *J. Org. Chem.*, **28**, 2385 (1963); H. Tanida, S. Teratake, Y. Hata, and M. Watanabe, *Tetrahedron Lett.*, 5341, 5345 (1969); L. A. Paquette, *J. Am. Chem. Soc.*, **92**, 5765 (1970); D. W. McNeil, M. E. Kent, E. Hedaya, P. F. D'Angelo, and P. O. Schlissel, *ibid.*, **93**, 3817 (1971); B. M. Trost and R. M. Cory, *ibid.*, **93**, 5573 (1971); J. A. Berson and R. F. Davis, *ibid.*, **94**, 3658 (1972); T. J. Katz and N. Acton, *ibid.*, **95**, 2738 (1973); B. M. Trost, R. M. Cory, P. H. Scudder, and H. B. Neubold, *ibid.*, **95**, 7813 (1973); D. R. James, G. H. Birnberg, and L. A. Paquette, *ibid.*, **96**, 7465 (1974); S. Masamune, N. Nakamura, and J. Spadaro, *ibid.*, **97**, 918 (1975); R. Askani, I. Gurang, and W. Schwertfeger, *Tetrahedron Lett.*, 1315 (1975); Y. C. Toong, W. T. Borden, and A. Gold, *ibid.*, 1549 (1975); D. M. Stout, T. Takaya, and A. I. Meyers, *J. Org. Chem.*, **40**, 563 (1975).
(4) (a) R. G. Bergmann, "Free Radicals", Vol. I, J. K. Kochi, Ed., New York, N.Y., (1973), pp 191-273, and references therein; C. R. Watson, R. M. Pagni, J. R. Dodd, and J. E. Bloor, *J. Am. Chem. Soc.*, **98**, 2551 (1976); T. C. Clarke, L. A. Wendling and R. G. Bergmann, *ibid.*, **97**, 5640 (1975); (b) P. S. Engel and D. J. Bishop, *ibid.*, **97**, 6754 (1975); P. B. Dervan and T. Uyehara, *ibid.*, **98**, 2003 (1976); (c) R. J. Crawford and M. Ohno, *Can. J. Chem.*, **52**, 3134 (1974); M. Schneider and H. Strohäcker, *Tetrahedron*, **32**, 619 (1976).
(5) (a) A. B. Evnin, D. R. Arnold, L. A. Karnischky, and E. Strom, *J. Am. Chem. Soc.*, **92**, 6218 (1970); (b) P. Dowd, *Acc. Chem. Res.*, **5**, 242 (1972); J. A. Berson, C. D. Duncan, and L. R. Corwin, *J. Am. Chem. Soc.*, **96**, 6175 (1974); J. A. Berson, L. R. Corwin, and J. H. Davis, *ibid.*, **96**, 6177 (1974); M. S. Platz, J. M. McBride, R. D. Little, J. J. Harrison, A. Shaw, S. E. Potter, and J. E. Berson, *ibid.*, **98**, 572, (1976); R. J. Baseman, D. W. Pratt, M. Chow, and P. Dowd, *ibid.*, **98**, 5726 (1976); (c) H. E. Zimmermann, R. J. Boettcher, N. E. Buehler, and G. E. Keck, *ibid.*, **97**, 5635 (1975).
(6) N. Rieber, J. Alberts, J. A. Lipsky, and D. M. Lemal, *J. Am. Chem. Soc.*, **91**, 5668 (1969).
(7) J. A. Berson and S. S. Olin, *J. Am. Chem. Soc.*, **91**, 777 (1969).
(8) D. M. Lemal and S. D. McGregor, *J. Am. Chem. Soc.*, **88**, 1335 (1966); L. A. Carpino, *Chem. Commun.*, 494 (1966).
(9) (a) E. L. Allred and J. C. Hinshaw, *Chem. Commun.*, 1021 (1969); (b) E. L. Allred, J. C. Hinshaw, and A. L. Johnson, *J. Am. Chem. Soc.*, **91**, 3382 (1969); E. L. Allred and A. L. Johnson, *ibid.*, **93**, 1300 (1971); (c) R. Askani, *Tetrahedron Lett.*, 3349 (1970); R. M. Moriarity, C.-L. Yeh, and N. Ishibi, *J. Am. Chem. Soc.*, **93**, 3085 (1971); (d) L. A. Paquette and M. J. Epstein, *ibid.*, **95**, 6717 (1973).
(10) J. A. Berson and S. S. Olin, *J. Am. Chem. Soc.*, **92**, 1086 (1970).
(11) J. A. Berson, E. W. Petrillo, Jr., and P. Bickart, *J. Am. Chem. Soc.*, **96**, 636 (1974).
(12) J. A. Berson, S. S. Olin, E. W. Petrillo, Jr., and P. Bickart, *Tethedron*, **30**, 1639 (1974).
(13) H. Olsen and J. P. Snyder, *J. Am. Chem. Soc.*, **96**, 7839 (1974).
(14) J. P. Snyder, V. T. Bandurco, F. Darack, and H. Olsen, *J. Am. Chem. Soc.*, **96**, 5158 (1974).
(15) Benzo derivatives of the unsaturated [2.2.1] azo *N*-oxide system **13** require temperatures around 180 °C in order to promote N_2O extrusion: W. R. Dolbier, L. McCullagh, D. Rolison, and K. E. Anapolle, *J. Am. Chem. Soc.*, **97**, 934 (1975).
(16) F. D. Greene and S. S. Hecht, *Tetrahedron Lett.*, 575 (1969); J. P. Snyder and V. T. Bandurco, *ibid.*, 4643 (1969); J. P. Snyder, L. Lee, and D. G. Farnum, *J. Am. Chem. Soc.*, **93**, 3816 (1971); P. Singh, *J. Org. Chem.*, **40**, 1405 (1975).
(17) (a) J. P. Snyder, L. Lee, V. T. Bandurco, C. Y. Yu, and R. J. Boyd, *J. Am. Chem. Soc.*, **94**, 3260 (1972); (b) J. P. Snyder, M. L. Heymann, and E. N. Suciu, *J. Org. Chem.*, **40**, 1395 (1975).
(18) J. Swigert and K. G. Taylor, *J. Am. Chem. Soc.*, **93**, 7337 (1971); K. G. Taylor and T. Riehl, *ibid.*, **94**, 250 (1972), and references therein.
(19) These absorptions have been assigned to the NO and NN stretches, respectively: N. B. Colthup, C. H. Daly, and S. E. Wiberley, "Introduction to Infrared and Raman Spectroscopy", Academic Press, New York, N.Y. 1964, pp 288-289.
(20) J. Kuhn, W. Hug, R. Geiger, and G. Wagniere, *Helv. Chim. Acta*, **54**, 2260 (1971).
(21) B. T. Gillis and P. E. Beck, *J. Org. Chem.*, **28**, 3177 (1963); R. Askani, *Chem. Ber.*, **98**, 2551 (1965).
(22) R. Askani, *Chem. Ber.*, **102**, 3304 (1969).
(23) C. R. Flynn and J. Michl, *J. Am. Chem. Soc.*, **95**, 5802 (1973).
(24) G. Herzberg and C. Reid, *Discuss. Faraday Soc.*, **9**, 92 (1950).
(25) J. M. Sandri, *J. Am. Chem. Soc.*, **81**, 320 (1959); E. F. Cox, M. C. Caserio, H. Hart, M. S. Silver, and J. D. Roberts, *ibid.*, **83**, 2720 (1961).
(26) J. D. Roberts and R. H. Mazur, *J. Am. Chem. Soc.*, **73**, 2509 (1951); C. G. Bergstrom and S. Siegel, *ibid.*, **74**, 145, 254 (1952).
(27) E. M. Engler, J. D. Andose, and P. v. R. Schleyer, *J. Am. Chem. Soc.*, **95**, 8005 (1973).
(28) M. J. Perkins and P. Ward, *Chem. Commun.*, 1134 (1971).
(29) J. C. Martin, J. E. Schultz, and J. W. Timberlake, *Tetrahedron Lett.*, 4629 (1967); J. C. Martin and J. W. Timberlake, *J. Am. Chem. Soc.*, **92**, 978 (1970); M. T. Liu and D. H. Chien, *J. Chem. Soc., Perkin Trans 2*, 937 (1974); B. K. Bandlish, A. W. Garner, M. L. Hodges, and J. W. Timberlake, *J. Am. Chem. Soc.*, **97**, 5856 (1975).
(30) H. Olsen, unpublished work.
(31) K. W. Egger, D. M. Golden, and S. W. Benson, *J. Am. Chem. Soc.*, **86**, 5420 (1964).
(32) H. M. Frey and A. Krantz, *J. Chem. Soc. A*, 1159 (1969); K. W. Egger and M. Jola, *Int. J. Chem. Kinet.*, **2**, 265 (1970).
(33) R. Hoffmann, *J. Am. Chem. Soc.*, **90**, 1475 (1968); J. A. Berson, L. D. Pedersen, and B. K. Carpenter, *ibid.*, **98**, 122 (1976), and references therein.
(34) J. B. Lisle, L. F. Williams, and D. E. Wood, *J. Am. Chem. Soc.*, **98**, 227 (1976); P. J. Krusic and P. Meakin, *ibid.*, **98**, 228 (1976).
(35) H. F. Schaefer III, *J. Am. Chem. Soc.*, **96**, 3754 (1974); J. H. Davis, D. R. Yarkony, and W. A. Goddard III, *ibid.*, **98**, 303 (1976).
(36) G. Steiner and R. Huisgen, *J. Am. Chem. Soc.*, **95**, 5056 (1973).
(37) (a) C. A. Eckert, *Ind. Eng. Chem.*, **59**, 20 (1967); K. F. Wong and C. A. Eckert, *Ind. Eng. Chem.*, **8**, 568 (1969); (b) M. H. Abraham, *Prog. Phys. Org. Chem.*, **11**, 1 (1974).
(38) R. Huisgen and W. E. Konz, *J. Am. Chem. Soc.*, **92**, 4102 (1973).
(39) L. Glasstone, K. J. Laidler, and H. Eyring, "The Theory of Rate Processes", McGraw-Hill, New York, N.Y., 1944, p 419; E. Amis, "Solvent Effects on Reaction Rates and Mechanisms", Elsevier, New York, N.Y., 1952.
(40) J. G. Kirkwood, *J. Chem. Phys.*, **2**, 351 (1934); cf. C. J. F. Böttcher, "Theory of Electrical Polarization", Elsevier, New York, N.Y., 1952.
(41) Dr. C. Larsen, University of Copenhagen, unpublished work.
(42) The molecular and transition state volumes given in the text include van der Waal's radii of 1.5 and 2.4 Å for H and O, respectively. If the nuclear coordinates are taken as the periphery of the idealized molecular sphere, $\mu_\pm$ = 5.1 D is obtained. The actual value can be considered to lie between the 1.7 and 5.1 D extremes probably in the vicinity of 2–2.5 D.
(43) R. C. Petersen, J. H. Markgraff, and S. D. Ross, *J. Am. Chem. Soc.*, **83**, 3819 (1961).
(44) O. Exner, *Prog. Phys. Org. Chem.*, **10**, 411 (1973).
(45) J. R. Leffler, *J. Org. Chem.*, **20**, 1202 (1955).
(46) J. P. Snyder and D. N. Harpp, *J. Am. Chem. Soc.*, **98**, 7821 (1976).
(47) R. Huisgen, *Angew. Chem.*, **75**, 742 (1963).
(48) The relative rates were calculated on the basis that **49** decomposes to N_2 and cyclohexadiene at −78 °C with $t_{1/2} \leq 30$ s[6] implying an $E_a \leq 14.2$ kcal/mol. A $\Delta S^\ddagger = +5.0$ eu has been assumed from the kinetic results for **48**.[46]
(49) E. Heilbronner, *Isr. J. Chem.*, **10**, 143 (1972).
(50) A. Yokozeki and K. Kuchitsu, *Bull. Chem. Soc. Jpn.*, **44**, 2356 (1971), and references therein.
(51) A. Yokozeki and K. Kuchitsu, *Bull. Chem. Soc. Jpn.*, **44**, 1783 (1971).
(52) E. L. Allred and K. J. Vorhees, *J. Am. Chem. Soc.*, **95**, 620 (1973).
(53) E. L. Allred and J. C. Hinshaw, *Tetrahedron Lett.*, 387 (1972).
(54) D. S. Glass, J. Zirner, and S. Winstein, *Proc. Clhem. Soc.*, 276 (1963); E. Vogel, H. Kiefer, and W. R. Roth, *Angew. Chem.*, **76**, 432 (1964); R. Huisgen, F. Mietzsch, G. Boche, and H. Seidl, *Chem. Soc., Spec. Publ.*, **No. 19**, 3 (1965).
(55) T. Ottersen, C. Romming, and J. P. Snyder, *Acta Chem. Scand., Ser. B*, **30**, 407 (1976).
(56) M. Sakai, *Tetrahedron Lett.*, 2297 (1973).
(57) G. Kretschmer, I. W. McCay, M. N. Paddon-Row, and R. N. Warrener, *ibid.*, 1339 (1975).
(58) P. v. R. Schleyer, J. E. Williams, and K. L. Blanchard, *J. Am. Chem. Soc.*, **92**, 2377 (1970).
(59) R. J. Boyd and M. A. Whitehead, *J. Chem. Soc., Dalton Trans.*, 73, 78, 82

(1972).
(60) J. W. McIver, Jr., *Acc. Chem. Res.*, 7, 72 (1974); M. J. S. Dewar and S. Kirschner, *J. Am. Chem. Soc.*, **96**, 6809 (1974); H. Metiu, J. Ross, and R. Silbey, *J. Chem. Phys.*, **61**, 3200 (1974).
(61) R. C. Bingham, M. J. S. Dewar, and D. H. Lo, *J. Am. Chem. Soc.*, **97**, 1285 (1975); **97**, 1294 (1975).
(62) N. L. Allinger and J. T. Sprague, *J. Am. Chem. Soc.*, **94**, 5734 (1972).
(63) "Organic Syntheses", Collect. Vol. 2, 250 (1943).
(64) In our preliminary report[13] the temperature was incorrectly given as 52.0°C.

Photolysis of α-Peracetoxynitriles. 2.[1] A Comparison of Two Synthetic Approaches to 18-Cyano-20-ketosteroids

Robert W. Freerksen, W. Edward Pabst, Michael L. Raggio, Steven A. Sherman, Randall R. Wroble, and David S. Watt*

Contribution from the Department of Chemistry, University of Colorado, Boulder, Colorado 80309. *Received August 25, 1976*

Abstract: A new photochemical reaction was utilized to functionalize unactivated carbon–hydrogen bonds in the C-18 angular methyl group in steroids. The photolysis of 20-peracetoxy-20-cyanosteroids derived from 17-ketosteroids furnished 18-cyano-20-ketosteroids. For example, the following sequence of reactions was applied to 3β-hydroxyandrost-5-en-17-one (**11**): (1) protection of the hydroxyl group in **11** using isobutylene–sulfuric acid to furnish 3β-*tert*-butoxyandrost-5-en-17-one (**12**), 73% yield; (2) condensation of **12** with the anion of 2-(diethylphosphono)propionitrile to afford 3β-*tert*-butoxy-20-carbonitrilepregna-5,17(20)-diene (**13**), 74% yield; (3) magnesium in methanol reduction of **13** to provide 3β-*tert*-butoxy-20-carbonitrilepregn-5-ene (**14**), 85% yield; (4) sequential treatment of **14** with lithium diisopropylamide, oxygen gas, and acetyl chloride to obtain 3β-*tert*-butoxy-20-carbonitrile-20-peracetoxypregn-5-ene (**15**), 62% yield; and (5) the photolysis of **15** to furnish 3β-*tert*-butoxy-18-carbonitrilepregn-5-en-20-one (**16**), 46% yield. In the same manner, 20-carbonitrile-20-peracetoxypregn-5-en-3-one ethylene ketal (**22**) afforded 18-carbonitrilepregn-5-ene-3,20-dione 3-ethylene ketal (**23**) in 21% yield, and 20-carbonitrile-3-methoxy-20-peracetoxy-19-norpregna-1,3,5(10)-triene (**31**) furnished 18-carbonitrile-3-methoxy-19-norpregna-1,3,5(10)-trien-20-one (**33**) in 39% yield. Finally, the new photochemical approach to 18-cyano-20-ketosteroids was contrasted with the cyanohydrin–ketonitrile reaction developed by Kalvoda.

Introduction

In recent years, a variety of ingenious synthetic methods have been developed to functionalize unactivated carbon–hydrogen bonds in steroids.[2] The impetus for such investigations was provided, in part, by the occurrence of the relatively rare mineralcorticosteroid, aldosterone (**1**). Apart from the

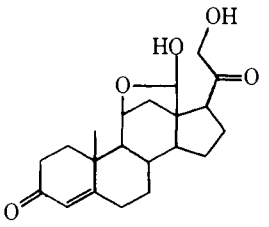

1

total synthesis[3] of **1**, a particular limitation in the partial synthesis of **1** was the limited availability of naturally occurring steroids bearing oxygen functionality at C-11 and C-18.

An examination of the functionality in aldosterone (**1**) revealed the 1,4 relationship of the oxygen substituents at C-11, C-18, and C-20. We were attracted to the possibility of introducing this functionality in a sequential fashion starting with a steroid functionalized only at C-20. To achieve this objective, we required a reiterative reaction in which a parent functional group (X) would migrate down the backbone of the steroid nucleus regioselectively and leave behind a daughter functional group (Y). A schematic representation of this process is shown below.

Results and Discussion

Recently, we reported[1] that the photolysis of α-peracetoxynitriles **3** derived from secondary nitriles **2** provided δ-ketonitriles **4** (Table I). This new photochemical reaction possessed the reiterative feature crucial to the success of the scheme outlined above. For example, the α-peracetoxynitrile

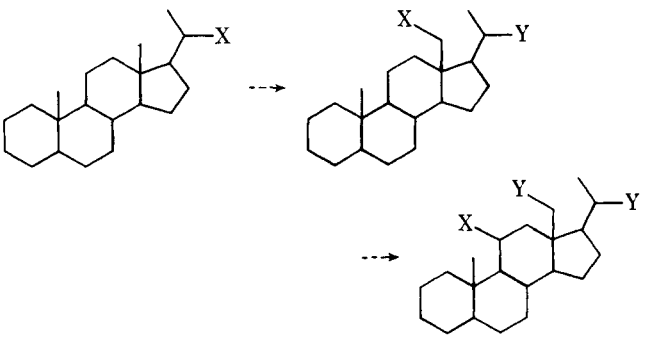

6 obtained from 2-phenylnonanenitrile (**5**) was photolyzed to provide the δ-ketonitrile **7**. To confirm the regioselectivity of this process, **7** was independently synthesized by alkylating hexanenitrile with β-bromopropiophenone ethylene ketal and hydrolyzing the ethylene ketal. A second peracetoxy group was introduced in the ketal nitrile **8** and the α-peracetoxynitrile **9** was photolyzed to obtain the δ-ketonitrile **10** in which the cyano group of **5** had clearly undergone two successive δ migrations. The only variation in this regioselectivity was observed in the photolysis of δ-peracetoxynitrile **3r** which afford the ε-ketonitrile **4r**.

Having developed a reaction which incorporated a reiterative feature as well as a high degree of regioselectivity, we returned to the objective of functionalizing unactivated carbon–hydrogen bonds in steroid systems. We now wish to report the first phase of our application of this reaction to function-